

2,5-diamino-6-ribitylamino-4(3*H*)-pyrimidinone 5'-phosphate synthases of fungi and archaea

Werner Römisch-Margl^{1,2}, Wolfgang Eisenreich¹, Ilka Haase³, Adelbert Bacher¹ and Markus Fischer³

- 1 Lehrstuhl für Organische Chemie und Biochemie, Technische Universität München, Garching, Germany
- 2 Institute of Bioinformatics and Systems Biology, Helmholtz Zentrum München, Neuherberg, Germany
- 3 Institute of Food Chemistry, University of Hamburg, Germany

Kevwords

2,5-diamino-6-ribitylamino-4(3*H*)-pyrimidinone 5'-phosphate synthase; archaea; fungi; riboflavin biosynthesis; stereochemistry

Correspondence

M. Fischer, Institut für Lebensmittelchemie, Universität Hamburg, Grindelallee 117, D-20146 Hamburg, Germany Fax: +49 40 428384342

Tel: +49 40 428384359

E-mail: markus.fischer@uni-hamburg.de

(Received 18 April 2008, revised 21 June 2008, accepted 4 July 2008)

doi:10.1111/j.1742-4658.2008.06586.x

The pathway of riboflavin (vitamin B₂) biosynthesis is significantly different in archaea, eubacteria, fungi and plants. Specifically, the first committed intermediate, 2,5-diamino-6-ribosylamino-4(3H)-pyrimidinone 5'-phosphate, can either undergo hydrolytic cleavage of the position 2 amino group by a deaminase (in plants and most eubacteria) or reduction of the ribose side chain by a reductase (in fungi and archaea). We compare 2,5-diamino-6ribitylamino-4(3H)-pyrimidinone 5'-phosphate synthases from the yeast Candida glabrata, the archaeaon Methanocaldococcus jannaschii and the eubacterium Aquifex aeolicus. All three enzymes convert 2,5-diamino-6ribosylamino-4(3H)-pyrimidinone 5'-phosphate into 2,5-diamino-6-ribitylamino-4(3H)-pyrimidinone 5'-phosphate, as shown by ¹³C-NMR spectroscopy using $[2,1',2',3',4',5'^{-13}C_6]2,5$ -diamino-6-ribosylamino-4(3H)-pyrimidinone 5'-phosphate as substrate. The β anomer was found to be the authentic substrate, and the α anomer could serve as substrate subsequent to spontaneous anomerisation. The M. jannaschii and C. glabrata enzymes were shown to be A-type reductases catalysing the transfer of deuterium from the 4(R) position of NADPH to the 1' (S) position of the substrate. These results are in agreement with the known three-dimensional structure of the M. jannaschii enzyme.

The coenzymes FMN and FAD derived from vitamin B_2 are essential in all organisms. They are involved in a wide variety of redox processes, some of which are fundamental to central energy transduction functions. They are also involved in a variety of non-redox processes such as DNA photorepair, blue-light sensing in plants and a variety of enzyme reactions including certain dehydration and isomerisation reactions [1–3]. In view of the vital role of these coenzymes, it appears likely that biosynthesis of the parent compound, vitamin B_2 (riboflavin, compound $\bf 8$ in Fig. 1), must already have been operative in the early phase of evolution.

The pathway of riboflavin biosynthesis has been studied in considerable detail for more than five decades (for review, see [4–7]). One of the driving forces for this research was the commercial requirement for bulk amounts (approximately 3000 tonnes per year) of

the vitamin for use in human and animal nutrition and as a non-toxic food colorant [8]. However, fermentation processes using yeasts and eubacteria have now completely replaced chemical synthesis of the trace nutrient [9].

The biosynthesis of the vitamin is summarised in Fig. 1. Although the final part of the pathway is universal in all organisms studied to date, the early section shows significant differences between taxonomic kingdoms. In eubacteria, fungi and plants, the first committed step, catalysed by the enzyme GTP cyclohydrolase II (reaction **A** in Fig. 1), consists of hydrolytic opening of the imidazole ring of GTP (compound **1** in Fig. 1) with concomitant removal of a pyrophosphate moiety; the reaction mechanism for this enzyme has been studied in considerable detail [10–13]. In archaea, the first committed step involves release of pyrophosphate and opening of the imidazole ring

Fig. 1. Biosynthesis of riboflavin. GTP cyclohydrolase II (A), GTP cyclohydrolase III (B), unknown enzyme (C), deaminase (D, G), reductase (E, F), terminal enzymes of the pathway (H). The biosynthetic pathway proceeds via reactions D and E in eubacteria and plants and via reactions F and G in yeasts. **1**, GTP; **2**, 2-amino-5-formylamino-6-ribosylamino-4(3H)-pyrimidinone 5'-phosphate; **3**, 2,5-diamino-6-ribosylamino-4(3H)-pyrimidinone 5'-phosphate; **5**, 2,5-diamino-6-ribitylamino-4(3H)-pyrimidinone 5'-phosphate; **5**, 2,5-diamino-6-ribitylamino-2,4(1H,3H)-pyrimidinedione 5'-phosphate; **7**, 3,4-dihydroxy-2-butanone 4-phosphate; **8**, riboflavin. Reaction **F**, catalysed by the reductases from *Methanocaldococcus jannaschii*, *Candida glabrata* and *Aquifex aeolicus*, is shown in the box.

of GTP, but without release of formate, under the catalytic influence of GTP cyclohydrolase III (reaction **B** in Fig. 1) [14]. The resulting formamide derivative (compound **2**) must then be deformylated to compound **3** in a process that is still incompletely understood (reaction **C** in Fig. 1).

The committed intermediate 3 undergoes position 2 deamination, producing compound 4 in plants and most eubacteria (reaction **D** in Fig. 1). However, com-

pound 3 is subject to side-chain reduction in fungi, producing the ribitol derivative 5 in fungi (reaction F in Fig. 1). In yeasts, the enzyme for the reduction reaction is named RIB7. Recently, the reaction catalysed by that enzyme has also been shown to occur in archaea (the corresponding enzyme is designated archaeal RIB7 throughout). [15,16]. The intermediates 4 and 5 of the two divergent pathways are then converted to compound 6 (reactions E and G, respec-

tively). It was found that the *ribD* gene of *Escherichia coli* and the *ribG* gene of *Bacillus subtilis* specify bifunctional proteins (RibD and RibG, respectively) that catalyse both reactions **D** and **E**. Intermediate **6** is further transformed into 6,7-dimethyl-8-ribityllumazine by condensation with 3,4-dihydroxybutanone 4-phosphate (compound **7**), mediated by 3,4-dihydroxybutanone 4-phosphate synthase (reaction **H** in Fig. 1). The resulting product is converted into a mixture of riboflavin (**8**) and the pathway intermediate **6** by a mechanistically unusual dismutation [17].

This paper describes the efficient expression, biochemical characterisation and comparison of 2,5-diamino-6-ribitylamino-4(3H)-pyrimidinone 5'-phosphate synthases (catalysing reaction F) from the yeast Candida glabrata (CglRED), the hyperthermophilic archaeon Methanocaldococcus jannaschii (MjaRED) and the hyperthermophilic eubacterium Aquifex aeolicus (AaeRED). NMR spectroscopy using chirally deuterated NADPH indicates that the M. jannaschii and C. glabrata enzyme are A-type reductases catalysing the transfer of deuterium from the 4(R) position of NADPH to the 1' (S) position of the substrate.

Results

Pyrimidine reductase families

Using the amino acid sequence of 2,5-diamino-6-ribitylamino-4(3H)-pyrimidinone 5'-phosphate synthase from A. aeolicus (AaeRED) as the template, all completely sequenced eubacterial, archaeal and fungi genomes in the public domain were screened for potential orthologues. Numerous microorganisms harbour two genes with significant similarity to the template sequence. More specifically, two similar genes were found in four of 45 fully sequenced archaeal genomes, with identities between 30 and 50% as compared to the search template (Candidatus Methanoregula boonei 6A8, Methanospirillum hungatei JF-1, Methanoculleus marisnigri JR1 and Methanocorpusculum labreanum Z).

Two orthologous proteins with identities from 21% to 37.5% were found in 16 of 547 fully sequenced eubacterial genomes. Most of the so-called RIB7-like proteins observed are devoid of one or more of the residues that are believed to be invariant for RIB7 and RibD proteins [18]. Four microorganisms with two sequences (Aquifex aeolicus VF5, (Pseudomonas syringae pv. tomato DC3000, Rubrobacter xylanophilus DSM 9941 and Xanthobacter autotrophicus Py2) were analysed in closer detail as shown in Fig. 2. All sequences of this group show the typical residues (indicated by asterisks) that are essential for the activity of

RibD- and RIB7-type proteins. Moreover, all sequences of the RibD protein group show the invariant residue Lys152 (*E. coli* numbering), which has been identified as a key residue for altering substrate specificity, with implications for the sequential order of the deaminase and reductase reactions in this pathway [18]. Yeast and fungal genomes show only the RIB7-type 2,5-diamino-6-ribitylamino-4(3*H*)-pyrimidinone 5'-phosphate synthase.

The putative genes were of two types, either with the two-domain architecture of the RibG protein of *Bacillus subtilis* or the RibD protein of *E. coli*, respectively [18–20], or the single-domain type of 2,5-diamino-6-ribitylamino-4(3*H*)-pyrimidinone 5'-phosphate synthase of *M. jannaschii* [16].

Enzyme preparation and quaternary structure

In order to provide a firm basis for functional comparison, we decided to clone and express the putative 2,5-diamino-6-ribitylamino-4(3H)-pyrimidinone 5'-phosphate synthase (single-domain type) of *C. glabrata* as well as the single-domain enzyme of *A. aeolicus* (encoded by a so-called *ribD2* gene). Due to their remarkable homology to fungal or archaeal RIB7 proteins, we designated this family RIB7-like proteins. Notably, *C. glabrata* is the most important human pathogenic yeast other than *Candida albicans*, and the species was selected for study with the view that the enzyme might have potential as an anti-mycotic drug target.

A recombinant *E. coli* strain harbouring a plasmid (pNCO-CglRED-H6) encoding the *C. glabrata* gene with a C-terminal hexahistidine tag under the control of a T5 promotor and a *lac* operator produced large amounts of a soluble recombinant protein with an apparent mass of 28.5 kDa as determined by SDS-PAGE.

A recombinant *E. coli* strain harbouring the native *ribD2* gene isolated from wild-type *A. aeolicus* in an expression plasmid under the control of a T5 promoter and *lac* operator produced only small amounts of the predicted RIB7-like protein. This was not surprising as the *A. aeolicus* gene comprises numerous codons that are known to be poorly transcribed in *E. coli*. To overcome this problem, a DNA segment specifying the amino acid sequence predicted by the *ribD2* gene was designed in order to optimise the conditions for expression in a heterologous *E. coli* host. Specifically, 73 codons (33%) were replaced in order to adapt the sequence to *E. coli* codon preferences, and 18 artificial restriction sites were introduced in order to facilitate future *in vitro* mutagenesis studies. The designed

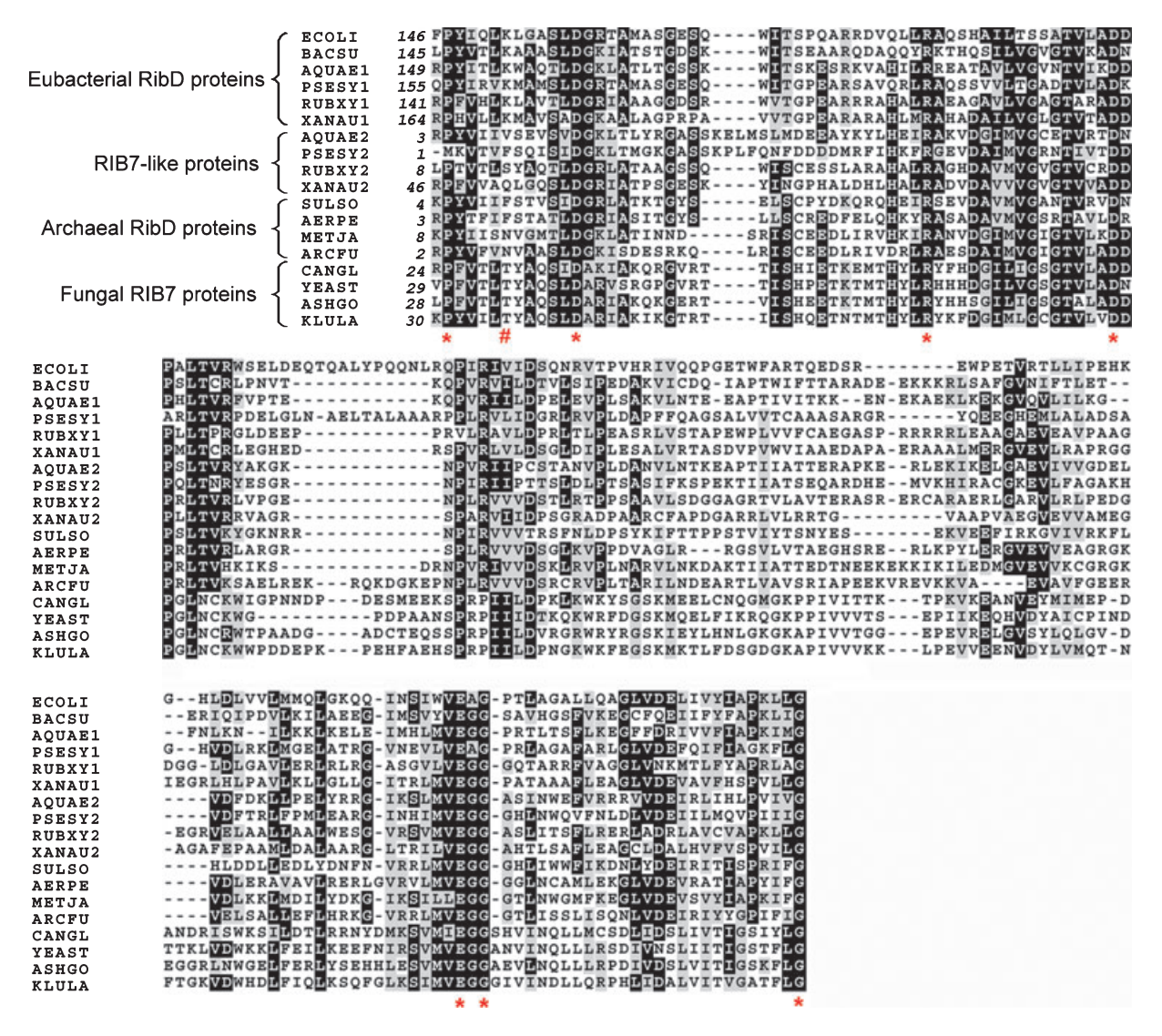


Fig. 2. Sequence comparison of putative eubacterial RibD protein domains (5-amino-6-ribitylamino-2,4(1H,3H)-pyrimidindione 5'-phosphate synthase), archaeal and fungal RIB7 proteins, and eubacterial RIB7-like protein domains (2,5-diamino-6-ribitylamino-4(3H)-pyrimidinone 5'-phosphate synthase). ECOLI, RibD protein of Escherichia coli (accession number P25539); BACSU, RibD protein of Bacillus subtilis (accession number P17618); AQUAE1, RibD protein of Aquifex aeolicus (accession number O66534); PSESY1, RibD protein of Pseudomonas syringae pv. tomato DC3000 (accession number NP_790537); RUBXY1, RibD protein of Rubrobacter xylanophilus DSM 9941 (accession number YP_644139); XANAU1, RibD protein of Xanthobacter autotrophicus Py2 (accession number YP_001419156); AQUAE2 (AaeRED), RIB7-like protein of A. aeolicus (accession number AAC06708); PSESY2, RIB7-like protein of Pseudomonas syringae pv. tomato DC3000 (accession number NP 790680): RUBXY2. RIB7-like protein of Rubrobacter xylanophilus DSM 9941 (accession number YP 645307): XA-NAU2, RIB7-like protein of Xanthobacter autotrophicus Py2 (accession number YP_001416938); SULSO, RIB7 protein of Sulfolobus solfataricus (accession number P95872); AERPE, RIB7 protein of Aeropyrum pernix K1 (accession number NP 147843); METJA (MiaRED), RIB7 protein of Methanocaldococcus jannaschii (accession number Q58085); ARCFU, RIB7 protein of Archaeoglobus fulgidus DSM 4304 (accession number O28272); CANGL (CgIRED), RIB7 protein of Candida glabrata (accession number Q6FU96); YEAST, RIB7 protein of Saccharomyces cerevisiae (accession number P33312); ASHGO, RIB7 protein of Ashbya gossypii (accession number Q757H6); KLULA, RIB7 protein of Kluyveromyces lactis (accession number Q6CJ61). Conserved residues are shown in black, homologous residues in grey. Invariant residues in RibD, RIB7 and RIB7-like proteins are marked by asterisks. Lysine 152 of the Escherichia coli RibD protein is marked by a hash. The figure was prepared using the program BOXSHADE.

sequence was assembled from 16 oligonucleotides by a sequence of eight PCR amplifications (Table S1 and Fig. S1) and cloned into the vector pNCO113, resulting

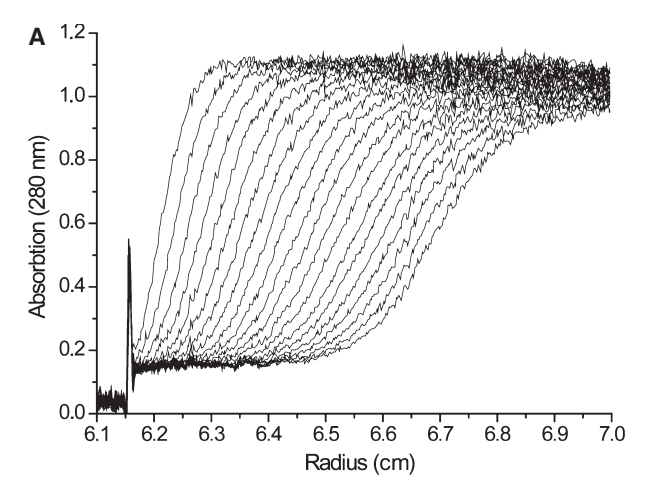
in the expression construct pNCO-AaeRED-syn. A recombinant *E. coli* M15[pREP4] strain harbouring this plasmid directed synthesis of a highly expressed protein

with an apparent mass of 25.3 kDa as determined by SDS-PAGE.

The recombinant proteins from C. glabrata and A. aeolicus were purified to apparent homogeneity as shown in Experimental procedures. The RIB7 protein of M. jannaschii was purified as described previously [16]. Velocity sedimentation of the recombinant proteins in the analytical ultracentrifuge showed single transients, indicating apparent sedimentation velocities of 3.8S for C. glabrata and 3.5S for A. aeolicus (Fig. 3A and Fig. S2A). Sedimentation equilibrium analysis indicated relative masses of 57.8 kDa (C. glabrata) and 50.6 kDa (A. aeolicus) (Fig. 3B and Fig. S2B). In light of the calculated subunit masses of 28.5 and 25.3 Da. respectively, these findings suggest homodimer structures. Similarly, the enzyme of M. jannaschii has been shown previously to sediment with an apparent velocity of 3.5S, and sedimentation equilibrium analysis indicated a relative mass of 50 kDa, which is close to the mass predicted for a homodimer [16].

Stereochemistry and kinetic properties

¹³C-NMR spectroscopy was used in order to monitor the catalytic activity of the recombinant proteins. Briefly, $[2,1',2',3',4',5'^{-13}C_6]$ -3 was prepared by treatment of [2,1',2',3',4',5'-13C₆]GTP with recombinant GTP cyclohydrolase II as described in Experimental procedures. As shown previously, the α and β anomers of compound 3 form an equilibrium mixture in aqueous solution at room temperature, and a dual set of ¹³C-NMR signals is therefore observed for each of the ¹³C-labelled carbon atoms of the ribosyl side chain [12]. Moreover, the signals of the sidechain carbon atoms of ¹³C-labelled compound 3 appear as multiplets due to ¹³C¹³C coupling. Treatment of the ¹³C-labelled substrate with the recombinant enzyme from M. jannaschii using NADPH as cosubstrate produced the NMR spectra shown in Fig. 4. The progressive disappearance of the substrate is accompanied by the appearance of a novel set of signals. Notably, the ¹³C-labelled position 2 pyrimidine carbon atom shows two singlet signals in the case of the substrate, which reflect the two anomers. In contrast, the position 2 pyrimidine carbon of the product shows only one singlet, as the compound is devoid of an anomeric carbon atom and does not form an equilibrium mixture (Figs 4 and 5). The series of multiplets in the range 44-73 p.p.m. represents the ¹³C-labelled ribityl side chain of product 5; the chemical shifts and ¹³C¹³C coupling constants (Table 1) are in line with that structure.



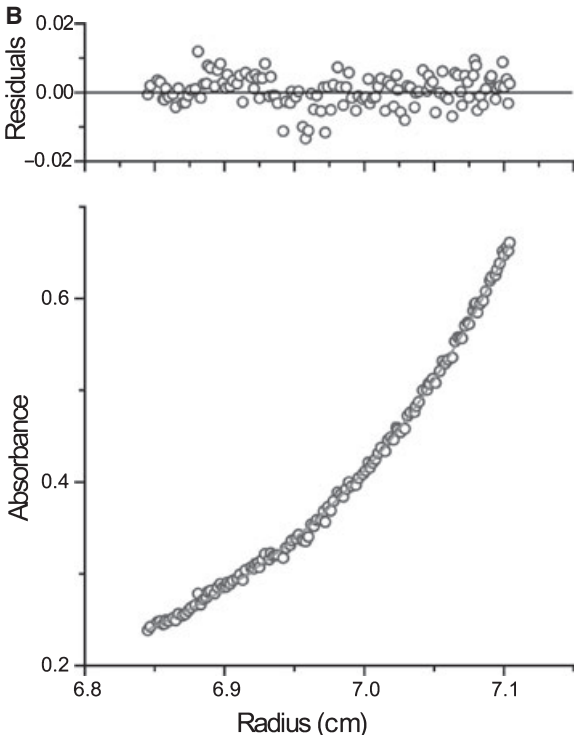


Fig. 3. (A) Boundary sedimentation of 2,5-diamino-6-ribitylamino-4(3H)-pyrimidinone 5'-phosphate synthase of *Aquifex aeolicus*. A solution containing 20 mM potassium phosphate, pH 7.0, 200 mM potassium chloride and 3.0 mg·mL⁻¹ protein was centrifuged at 55 000 \mathbf{g} (20 °C). The sample was scanned at intervals of 5 min. (B) Sedimentation equilibrium analysis of 2,5-diamino-6-ribitylamino-4(3H)-pyrimidinone 5'-phosphate synthase of *A. aeolicus*. A solution containing 20 mM potassium phosphate, pH 7.0, 200 mM potassium chloride and 0.4 mg·mL⁻¹ protein was centrifuged at 10 000 \mathbf{g} (4 °C). Residuals of the fitted data are shown at the top.

Quantitative analysis of the signal integrals reveals rapid consumption of the β anomer and less rapid consumption of the α anomer of substrate 3. All data are in line with the hypothesis that the β anomer serves as

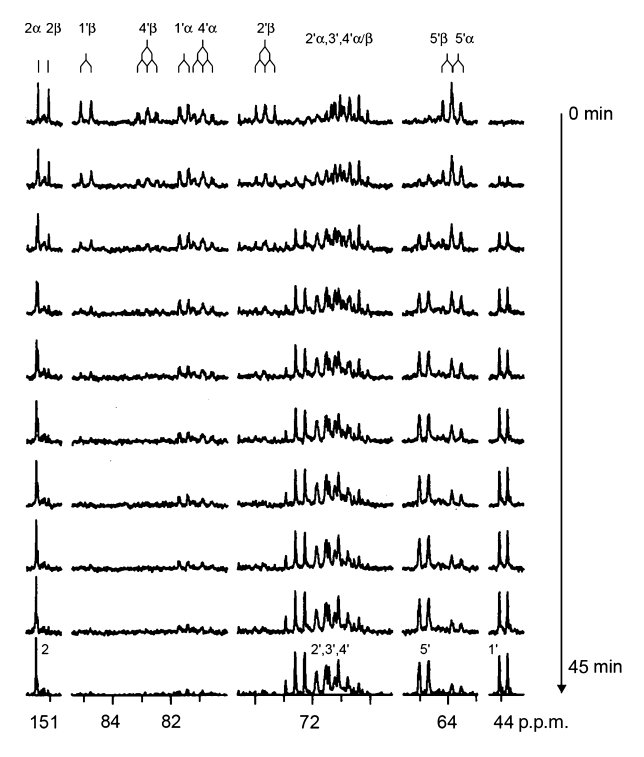


Fig. 4. Time-resolved $^{13}\text{C-NMR}$ signals. A mixture of [2,1′,2′,3′, 4′,5′- $^{13}\text{C}_6$]-**3**α and [2,1′,2′,3′,4′,5′- $^{13}\text{C}_6$]-**3**β was generated by incubation of a solution containing 5 mM [2,1′,2′,3′,4′,5′- $^{13}\text{C}_6$]GTP, 100 mM Tris/HCl pH 8.2, 10 mM MgCl₂, 10 mM dithiothreitol, 10% D₂O, 5 mM NADPH, 0.5 mM ATP, 5 mM phosphoenolpyruvate, 1 mg GTP cyclohydrolase II, 2 units of guanylate kinase and 2 units of pyruvate kinase in a total volume of 0.5 mL. 2,5-diamino-6-ribitylamino-4(3*H*)-pyrimidinone 5′-phosphate synthase from *Methanocaldococcus jannaschii* (0.14 mg) was added, and $^{13}\text{C-NMR}$ spectra were recorded at intervals of 5 min at 30 °C. The signals of **3**β disappear first in comparison with the **3**α anomer.

direct substrate of the reductase and can be progressively regenerated from the α anomer by spontaneous anomerisation.

Kinetic analysis of the recombinant proteins from C. glabrata and A. aeolicus was performed by

 13 C-NMR spectroscopy using [1- 13 C₁]-3 as the substrate (Fig. 6). The ¹³C-NMR spectrum of the substrate is characterised by two singlets at 85 and 82 p.p.m., reflecting the position 1' side-chain carbon atoms of the α and β anomers, respectively, that are present at equilibrium. Treatment of the substrate mixture with the recombinant 2.5-diamino-6-ribitylamino-4(3H)-pyrimidinone 5'-phosphate synthases using NADPH as cosubstrate results in progressive disappearance of substrate signals and the appearance of a singlet at 42 p.p.m., reflecting the 1' carbon of the ribityl side chain of product 5. Kinetic analysis confirmed preferential consumption of the β anomer of the substrate, which is progressively regenerated from the α anomer by spontaneous isomerisation (data not shown). The apparent catalytic rates of the recombinant enzymes from C. glabrata and A. aeolicus are 0.2 (37 °C) and 0.04 μmol mg⁻¹ min⁻¹ (57 °C), respectively (that for M. jannaschii is $0.8 \mu mol mg^{-1} min^{-1} (30 \,^{\circ}C)$ [16]).

Previously, we have shown by *in vivo* studies using the ascomycete *Ashbya gossypii* that biosynthesis of riboflavin involves introduction of a hydrogen atom into the 1'-proS position of the ribityl side chain [21]. However, no stereochemical information is available for biosynthesis of riboflavin in archaea. We used ¹³C-NMR spectroscopy and stereospecifically deuterated NADP²H in order to monitor introduction of deuterium into the 1' position under the catalytic influence of 2,5-diamino-6-ribitylamino-4(3*H*)-pyrimidinone 5'-phosphate synthases of archaeal and fungal origin.

Chirally deuterated NADP²H was generated *in situ*. More specifically, glucose dehydrogenases from *Thermoplasma acidophilum* or *Pseudomonas* sp. were used to generate 4(R)- and 4(S)-NADP²H, respectively, from [1-²H₁] glucose [22]. As shown in Fig. 7, reduction of [1'-¹³C₁]-3 using 4(S)-NADP²H and reductase from *M. jannaschii* gave a single ¹³C signal for the 1' carbon of product 5. However, using 4(R)-NADP²H

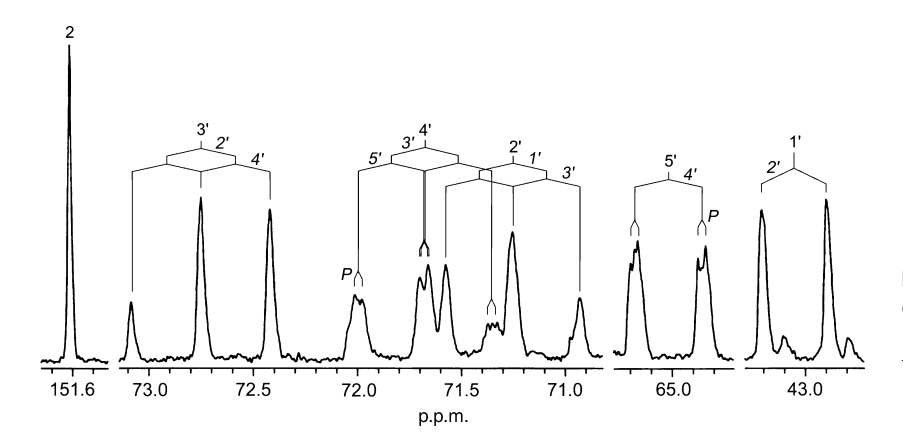


Fig. 5. ¹³C-NMR signals for product **5** obtained by treatment of [2,1',2',3',4',5'-¹³C₆]-**3** with the reductase from *Methanocaldococcus jannaschii*. ¹³C¹³C and ¹³C³¹P couplings are indicated. For details, see legend to Fig. 4.

Table 1. NMR data for $[2,1',2',3',4',5'^{-13}C_6]$ -2,5-diamino-6-ribitylamino-4(3*H*)-pyrimidinone 5'-phosphate (compound **5**) using D₂O as solvent.

Carbon	Chemical shift (p.p.m.)		Coupling constants (Hz)			
atom	¹ H	¹³ C	J _{CC}	J _{CP}	INADEQUATE	¹³ C-TOCSY
2		151.6				
1'-proS	3.30	43.0	39.1 (2')		2′	2',3',4',5'
1'-proR	3.46					
2'	3.77	71.2	40.5 (1',3')		1′	1′,3′,4′,5′
3′	3.55	72.7	41.6 (2',4')			1',2',4',5'
4′	3.70	71.7	41.6 (3') 40.2 (5')	5.1	5′	1′,2′,3′,5′
5′	3.74	65.0	40.6 (4')	4.5	4'	1′,2′,3′,4′

gave a pattern of four lines, consisting of a singlet at 42.7 p.p.m. and a triplet centred at 42.4 p.p.m., reflecting product molecules carrying one deuterium atom in the 1' position, which is conducive to an upfield shift of 0.3 p.p.m.; moreover, ²H¹³C coupling results in a triplet due to the quadrupole character of deuterium. These data show that the 4(R) hydrogen of NADPH is transferred by the *M. jannaschii* reductase.

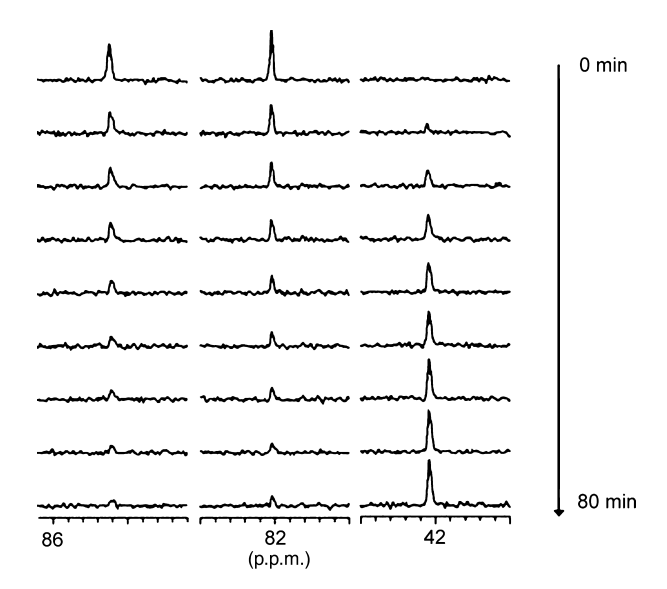


Fig. 6. Time-resolved $^{13}\text{C-NMR}$ signals. A mixture of [1′- $^{13}\text{C}_1$]-**3**α and [1′- $^{13}\text{C}_1$]-**3**β was generated by incubation of a solution containing 5 mm [1′- $^{13}\text{C}_1$]GTP, 100 mm Tris/HCl pH 8.2, 10 mm MgCl₂, 10 mm dithiothreitol, 10% D₂O, 5 mm NADPH, 0.5 mm ATP, 5 mm phosphoenolpyruvate, 1 mg GTP cyclohydrolase II, 2 units of guanylate kinase and 2 units of pyruvate kinase in a total volume of 0.5 mL. 2,5-diamino-6-ribitylamino-4(3*H*)-pyrimidinone 5′-phosphate synthase from *Aquifex aeolicus* (1.2 mg) was added, and $^{13}\text{C-NMR}$ spectra were recorded at intervals of 10 min at 57 °C.

Figure 8 shows a section from the HMQC spectrum of compound 5 obtained from [1',2',3',4',5'-\dangle^13-3] by treatment with the recombinant enzyme of *M. jannaschii*. The diastereotopic hydrogen atoms in the 1' position of the ribityl side chain showed correlation signals at 3.46 p.p.m. (1'-proR) and 3.30 p.p.m. (1'-proS) [21]. A similar experiment using deuterated 4(R)-NADP²H gave an HMQC spectrum with a correlation signal for 1' at 3.43 p.p.m. only (data not shown). The upfield-shifted signal for the second hydrogen at carbon 1' was not observed. We conclude that the hydrogen atom resonating at 3.30 p.p.m. (1'-proS) [21] is contributed by the cosubstrate NADP²H.

Experiments with recombinant 2,5-diamino-6-ribitylamino-4(3H)-pyrimidinone 5'-phosphate synthase from C. glabrata using $[1',2',3',4',5'-^{13}C_5]$ -3 and 4R-NADP²H gave HMQC spectra with the same signal pattern, indicating that the yeast enzyme shows the same stereospecificity with respect to hydrogen introduction into the 1' side-chain position as the archaeal reductase.

Discussion

In line with the multiple sequence alignments (Fig. 2 and Fig. S3), we show that the enzymes specified by the RIB7 genes of yeast, C. glabrata and the archaeon M. jannaschii can catalyse reduction of the GTP cyclohydrolase II product, compound 3, without prior ring deamination. Moreover, the enzyme specified by the exceptional, monofunctional reductase from the hyperthermophilic eubacterium A. aeolicus is shown to catalyse the same reaction. This protein shows 42% identity with the RIB7 protein from M. jannaschii (94 identical amino acids) and 19% identity with the protein from C. glabrata (50 identical residues; Fig. S3). Seven amino acid residues appear to be absolutely conserved between both major reductase classes (RibD and RIB7 class). A major distinguishing feature, however, is the invariable presence of a lysine residue at position 152 (position reference to RibD of E. coli) in the eubacterial reductases, whereas reductases from archaea and fungi carry various amino acid residues in that position [18]. This invariant lysine residue at position 152 (marked by a hash in Fig. 2) is believed to contribute to the substrate specificity of RibD proteins. This residue is not present in archaeal and yeast RIB7-like proteins and eubacterial RIB7like proteins.

It should be noted that bifunctional as well as monofunctional reductases have been shown to occur in eubacteria. In the bifunctional enzymes, the deaminase domain usually occupies the N-terminal position.

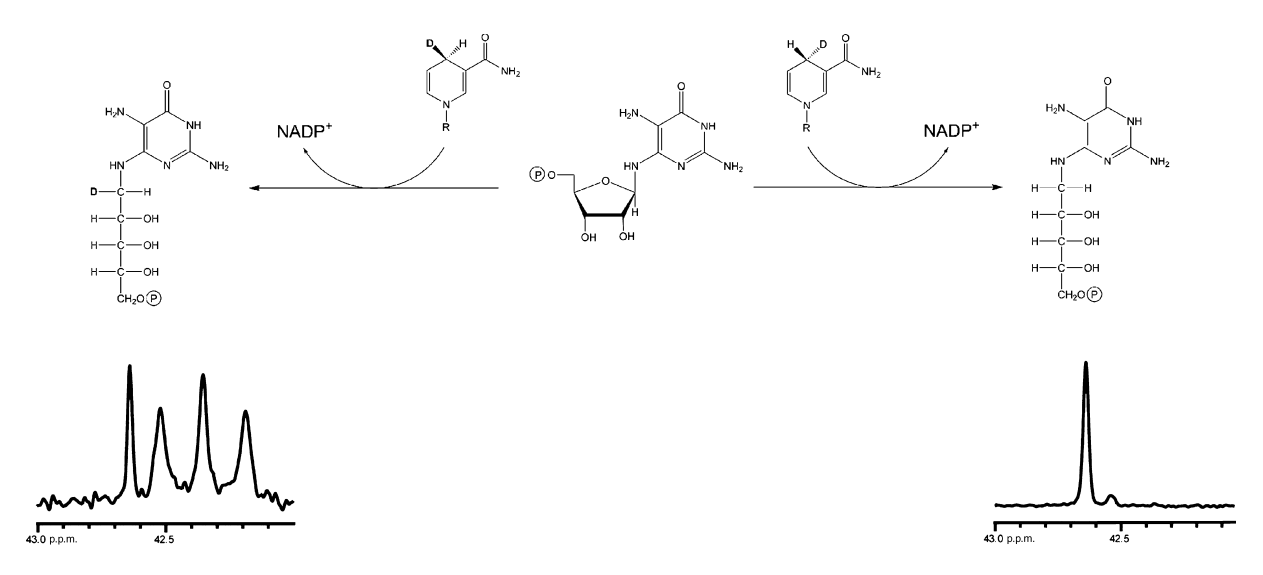


Fig. 7. Stereochemistry of hydride transfer from NADPH to the product of the *Methanocaldococcus jannaschii* reductase. Chirally deuterated NADPH was generated from [1-²H]glucose. Only deuterium from the 4(R) position of NADPH is transferred into the 1'-proS position of product **5** (left side). ¹³C-NMR signals of the 1' carbon of product **5** are shown.

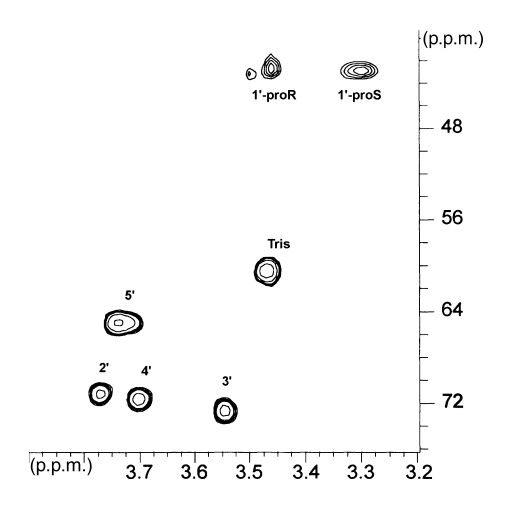


Fig. 8. Two-dimensional HMQC spectrum of $[1',2',3',4',5'^{-13}C_5]$ -**5.** The signal of the 1'-proS proton is absent if 4(R)-NADP²H is used as cosubstrate in the reaction with the reductases from *Methanocaldococcus jannaschii* or *Candida glabrata*.

In some cases [Streptomyces avermitilis MA-4680, accession number Q82FY3; Streptomyces coelicolor A3(2), accession number Q9RKM1; Nocardia farcinica, accession number Q5Z3S1], the reductase domain is located at the N-terminus and the predicted deaminase at the C-terminus of the bifunctional protein.

In plants, orthologues of pyrimidine reductases of the riboflavin pathway have not been characterised so far. On the basis of database searches, it has been assumed that putative plant pyrimidine reductase domains catalyse the equivalent reduction to RibD

proteins. In these proteins, the associated deaminase domains lack an invariant zinc-binding motif [18]. It has been shown experimentally that plants produce deaminases that use product 3 of GTP cyclohydrolase II as substrate [23]. This deaminase contains 1 equivalent of Zn²⁺ per subunit. Thus, the early part of the riboflavin biosynthetic pathway in plants is similar to that of eubacteria, rather than that in fungi and archaea. In view of the close similarity between putative plant deaminases and their apparently universal occurrence in all sequenced plant genomes, these orthologues must have arisen prior to the speciation of higher plants. The deaminase activity of the plant proteins could be assigned to the N-terminal part, but the C-terminal section was not able to catalyse the reduction equivalent to that catalysed by RibD proteins [23].

Studies using chirally deuterated NADP²H have identified the *M. jannaschii* and *C. glabrata* enzymes as A-type reductases. Previous studies had indicated that the proS hydrogen atom of the position 1' methylene group of the riboflavin side chain resonates at a higher field compared to the proR proton [21]. Based on that information, it was shown previously that reduction of the ribosyl side chain of compound 3 in the ascomycete *Ashbya gossypii* is conducive to introduction of a hydrogen atom into the 1'-proS position of the ribityl side chain of riboflavin [21]. We have extended these observations by *in vitro* studies using the pyrimidine reductases of *M. jannaschii* and *C. glabrata*. The position 1' hydrogen atom that resonates at a higher field

is introduced from NADPH by both enzymes in this study. Hence, the archaeal and the fungal enzyme operate with the same stereospecificity.

Experimental procedures

Materials

Restriction enzymes were obtained from New England Biolabs (Schwalbach, Germany). T4 DNA ligase was obtained from Gibco BRL (Karlsruhe, Germany). EXT DNA polymerase and Taq polymerase were obtained from Finnzymes (Epsoo, Finland). Oligonucleotides were synthesised by Thermo Electron GmbH (Ulm, Germany). A plasmid miniprep kit from PEQLab (Erlangen, Germany) was used for plasmid DNA isolation and purification. DNA fragments and PCR amplificates were purified using a gel extraction kit or Cycle Pure kit from PEQLab. Casein hydrolysate and yeast extract were obtained from Gibco BRL, and isopropyl-β-D-thiogalactoside was obtained from Biomol (Hamburg, Germany). $[1',2',3',4',5'^{-13}C_5]GTP$, [2,1',2',3',4',5'-13C₆]GTP and [1'-13C₁]GTP were prepared enzymatically from ¹³C-labelled glucose and xanthin by a modification of published procedures [24-27]. Recombinant GTP cyclohydrolase II of E. coli was prepared according to published procedures [28]. Recombinant 2,5-diamino-6-ribitylamino-4(3H)-pyrimidinone 5'-phosphate synthase from M. jannaschii was prepared as described previously [16].

Strains and plasmids

Escherichia coli strains and plasmids used in this study are summarised in Table S2. Cells were grown at 37 °C in LB medium containing 170 mg·L $^{-1}$ ampicillin and 15 mg·L $^{-1}$ kanamycin where appropriate.

Transformation

Ligation mixtures were transformed into *E. coli* XL1-Blue cells. Transformants were selected on LB solid medium supplemented with ampicillin. The plasmids were re-isolated and analysed by restriction analysis and DNA sequencing. The expression plasmid was then transformed into *E. coli* M15[pREP4] cells carrying the pREP4 repressor plasmid for overexpression of lac repressor protein. Kanamycin and ampicillin were used to secure the maintenance of both plasmids in the host strain.

Cloning of 2,5-diamino-6-ribitylamino-4(3H)-pyrimidinone 5'-phosphate synthase from *C. glabrata* (CgIRED)

The hypothetical open reading frame with accession number Q6FU96 was amplified by PCR using C. glabrata

chromosomal DNA as template and the oligonucleotides CglRED-EcoRI and CglRED-H6-HindIII as primers (Table S1). The amplificate was digested using *Eco*RI and *Hin*dIII and ligated into expression vector pNCO113 digested with the same enzymes, yielding the plasmid pNCO-CglRED-H6 (Table S2).

Preparation of a synthetic gene for 2,5-diamino-6-ribitylamino-4(3H)-pyrimidinone 5'-phosphate synthase from *A. aeolicus*

The partially complementary oligonucleotides AaeRED-1 and AaeRED-2 were annealed and treated with DNA polymerase. The resulting 101 bp segment was elongated by a series of seven PCR amplifications using pairwise combinations of oligonucleotides (Table S1 and Fig. S1). The resulting 721 bp DNA fragment was digested with *Eco*RI and *HindIII* and ligated into plasmid pNCO113 treated with the same restriction endonucleases, giving the expression plasmid pNCO-AaeRED-syn (Table S2).

Fermentation

The recombinant *E. coli* strain M15[pREP4] harbouring pNCO113 expression plasmids pNCO-CglRED-H6 or pNCO-AaeRED-syn was grown in LB medium containing ampicillin and kanamycin at 37 °C with shaking overnight. Erlenmeyer flasks containing 500 mL of medium were then inoculated at a ratio of 1 : 50 and incubated at 37 °C with shaking. At an attenuance of 0.6 (600 nm), isopropyl- β -D-thiogalactoside was added to a final concentration of 2 mM, and incubation was continued for 4 h. Cells were harvested by centrifugation (1500 g for 15 min at 4 °C) and stored at -20 °C.

Purification of 2,5-diamino-6-ribitylamino-4(3H)-pyrimidinone 5'-phosphate synthase from *C. glabrata*

The frozen cell mass of recombinant $E.\ coli$ strain M15[pREP4] harbouring pNCO-GglRED-H6 was thawed in 50 mM potassium phosphate, pH 8.0, containing 300 mM sodium chloride (buffer A). The suspension was ultrasonically treated and centrifuged (25 000 g for 10 min at 4 °C). The supernatant was placed on a column of nickel-chelating Sepharose (GE Healthcare Europe GmbH, Munich, Germany; 1.5×7 cm) that was subsequently washed with buffer A and developed with a gradient of 0–500 mM imidazole in buffer A. Fractions were combined and concentrated by ultrafiltration. The resulting solution was placed on top of a Superdex-200 column (GE Healthcare; 2.6×60 cm) and developed using buffer A. Fractions were combined and concentrated by ultrafiltration.

Purification of 2,5-diamino-6-ribitylamino-4(3H)pyrimidinone 5'-phosphate synthase from A. aeolicus

The frozen cell mass of recombinant E. coli strain M15[pREP4] harbouring pNCO-AaeRED-syn was thawed in 20 mm potassium phosphate containing 2 mm dithiothreitol (pH 7.0). The suspension was ultrasonically treated and centrifuged (25 000 g for 10 min at 4 °C). The supernatant was brought to 70 °C. After 5 min, the mixture was cooled to 10 °C and centrifuged (15 000 g, 20 min). The supernatant was placed on top of an HA Macroprep 45 µm column (45 mL, Amersham Biosciences) that had been equilibrated with 20 mm potassium phosphate, pH 7.0. The column was developed with a gradient from 20 mm to 1 m potassium phosphate. pH 7.0. Fractions were combined and concentrated by ultrafiltration. The supernatant was placed on top of a Superdex-200 column (GE Healthcare; 2.6 cm × 60 cm), which was then developed with 20 mm Tris/HCl pH 7.8, containing 100 mm potassium chloride and 5 mm dithiothreitol. Fractions were combined and concentrated by ultrafiltration using Amicon 10 kDa membranes (Millipore GmbH, Schwalbach, Germany).

Analytical ultracentrifugation

Experiments were performed using an Optima XL-A analytical ultracentrifuge from Beckman Instruments (Palo Alto, CA, USA) equipped with absorbance optics. Aluminium double sector cells equipped with quartz windows were used throughout. Sedimentation equilibrium experiments were performed with solutions containing buffer (*A. aeolicus*, 20 mM potassium phosphate, 200 mM potassium chloride, pH 7.0; *C. glabrata*, 100 mM potassium phosphate, pH 8.0) and 0.4 mg·mL⁻¹ protein at 10 000 *g* (*A. aeolicus*) or 12 500 *g* (*C. glabrata*) and 4 °C. Boundary sedimentation experiments were performed at 55 000 *g* and 20 °C using a solution containing buffer (see above) and 3.0 mg·mL⁻¹ protein. The partial specific volume was estimated from the amino acid composition, yielding values of 0.7531 mL·g⁻¹ (*A. aeolicus*) and 0.7379 mL·g⁻¹ (*C. glabrata*) [29].

NMR spectroscopy

¹H and ¹³C spectra were acquired using a DRX 500 spectrometer from Bruker (Karlsruhe, Germany) at transmitter frequencies of 500.13 and 125.76 MHz, respectively. Two-dimensional HMQC, INADEQUATE and TOCSY spectra were measured using standard Bruker software (XWINNMR 3.0). Composite pulse decoupling was used for ¹³C-NMR measurements. ³-(trimethylsilyl)propanesulfonate served as an external standard for ¹H- and ¹³C-NMR measurements.

Assay of 2,5-diamino-6-ribitylamino-4(3H)pyrimidinone 5'-phosphate synthase activity

Assay mixtures contained 100 mm Tris/HCl pH 8.2, 10 mm MgCl₂, 10 mm dithiothreitol, 10% D₂O, 5 mm NADPH, 0.5 mm ATP, 5 mm phosphoenolpyruvate, 5 mm ¹³C-labelled GTP, 1 mg GTP cyclohydrolase II, 2 units of guanylate kinase and 2 units of pyruvate kinase in a total volume of 0.5 mL, and were incubated for 30 min at 37 °C in order to generate the reductase substrate 3 (the addition of guanylate kinase and pyruvate kinase served to recycle GMP, a by-product of GTP cyclohydrolase II, into GTP). 2,5-diamino-6-ribitylamino-4(3*H*)-pyrimidinone 5′-phosphate synthase was added as required, and ¹³C-NMR spectra were recorded at a given temperature in intervals of 5 or 10 min respectively.

Multiple sequence alignment

We analysed 547 fully sequenced eubacterial genomes, 45 fully sequenced archaeal genomes and 15 fungal genomes from GenBank using the NCBI server with default settings for all input parameters (http://www.ncbi.nlm.nih.gov/sutils/genom_table.cgi). The RIB7-like protein from *A. aeolicus* was used as the query sequence. Based on this analysis and further sequences from Swiss-Prot, Fig. 2 and Fig. S3 were prepared using CLUSTAL w from the Kyoto University Bioinformatics Center (http://align.genome.jp/), using default options for all input parameters. The sequence alignment was edited using BOXSHADE from EMBL (http://www.ch.embnet.org/software/BOX form.html).

Acknowledgements

This work was supported by grants from the Deutsche Forschungsgemeinschaft (project number FI 824/1-1,2), the Fonds der Chemischen Industrie, and the Hans-Fischer-Gesellschaft e.V.

References

- Briggs WR, Beck CF, Cashmore AR, Christie JM, Hughes J, Jarillo JA, Kagawa T, Kanegae H, Liscum E, Nagatani A *et al.* (2001) The phototropin family of photoreceptors. *Plant Cell* 13, 993–997.
- 2 Müller F (1992) Chemistry and Biochemistry of Flavoenzymes. CRC Press, Boca Raton, FL.
- 3 Sancar A (2004) Photolyase and cryptochrome blue-light photoreceptors. *Adv Protein Chem* 69, 73– 100.
- 4 Bacher A, Eberhardt S & Richter G (1996) Biosynthesis of riboflavin. In *Escherichia coli and Salmonella ty-phimurium* (Neidhardt FC, Curtiss R, Ingraham JL, Linn ECC, Low KB, Magasanik B, Reznikoff WS,

- Riley M, Schaecter M & Umbarger HE, eds), pp. 657–664. ASM Press, Washington DC.
- 5 Fischer M & Bacher A (2005) Biosynthesis of flavocoenzymes. Nat Prod Rep 22, 324–350.
- 6 Fischer M & Bacher A (2006) Biosynthesis of vitamin B₂ in plants. *Physiol Plant* 126, 304–318.
- 7 Young DW (1986) The biosynthesis of the vitamins thiamin, riboflavin, and folic acid. *Nat Prod Rep* 3, 395– 419.
- 8 Wilska-Jeszka J (2007) Food colorants. In *Chemical and Functional Properties of Food Components* (Sikorski ZE, ed.), 3rd edn., pp. 245–274. CRC Press, Boca Raton, FL.
- 9 Stahmann KP, Revuelta JL & Seulberger H (2000) Three biotechnical processes using *Ashbya gossypii*, *Candida famata*, or *Bacillus subtilis* compete with chemical riboflavin production. *Appl Microbiol Biotechnol* **53**, 509–516.
- 10 Kaiser J, Schramek N, Eberhardt S, Puttmer S, Schuster M & Bacher A (2002) Biosynthesis of vitamin B₂. An essential zinc ion at the catalytic site of GTP cyclohydrolase II. Eur J Biochem 269, 5264–5270.
- 11 Ren J, Kotaka M, Lockyer M, Lamb HK, Hawkins AR & Stammers DK (2005) GTP cyclohydrolase II structure and mechanism. *J Biol Chem* **280**, 36912–36919.
- 12 Ritz H, Schramek N, Bracher A, Herz S, Eisenreich W, Richter G & Bacher A (2001) Biosynthesis of riboflavin: studies on the mechanism of GTP cyclohydrolase II. *J Biol Chem* **276**, 22273–22277.
- 13 Schramek N, Bracher A & Bacher A (2001) Biosynthesis of riboflavin. Single turnover kinetic analysis of GTP cyclohydrolase II. J Biol Chem 276, 44157–44162.
- 14 Graham DE, Xu H & White RH (2002) A member of a new class of GTP cyclohydrolases produces formylaminopyrimidine nucleotide monophosphates. *Biochemistry* **41**, 15074–15084.
- 15 Graupner M, Xu H & White RH (2002) The pyrimidine nucleotide reductase step in riboflavin and F(420) biosynthesis in archaea proceeds by the eukaryotic route to riboflavin. *J Bacteriol* **184**, 1952–1957.
- 16 Chatwell L, Krojer T, Fidler A, Romisch W, Eisenreich W, Bacher A, Huber R & Fischer M (2006) Biosynthesis of riboflavin: structure and properties of 2,5-diamino-6-ribosylamino-4(3H)-pyrimidinone 5'-phosphate reductase of *Methanocaldococcus jannaschii*. *J Mol Biol* 359, 1334–1351.
- 17 Fischer M & Bacher A (2008) Biosynthesis of vitamin B₂. Structure and mechanism of riboflavin synthase. *Arch Biochem Biophys* **474**, 252–265.
- 18 Stenmark P, Moche M, Gurmu D & Nordlund P (2007) The crystal structure of the bifunctional deaminase/reductase RibD of the riboflavin biosynthetic pathway in *Escherichia coli*: implications for the reductive mechanism. *J Mol Biol* 373, 48–64.

- 19 Richter G, Fischer M, Krieger C, Eberhardt S, Lüttgen H, Gerstenschläger I & Bacher A (1997) Biosynthesis of riboflavin: characterization of the bifunctional deaminase-reductase of *Escherichia coli* and *Bacillus subtilis*. *J Bacteriol* 179, 2022–2028.
- 20 Chen SC, Chang YC, Lin CH, Lin CH & Liaw SH (2006) Crystal structure of a bifunctional deaminase and reductase from *Bacillus subtilis* involved in riboflavin biosynthesis. *J Biol Chem* 281, 7605–7613.
- 21 Keller PJ, Le Van Q, Kim SU, Bown DH, Chen HC, Kohnle A, Bacher A & Floss HG (1988) Biosynthesis of riboflavin: mechanism of formation of the ribitylamino linkage. *Biochemistry* 27, 1117–1120.
- 22 Mostad SB, Helming HL, Groom C & Glasfeld A (1997) The stereospecificity of hydrogen transfer to NAD(P)⁺ catalyzed by lactol dehydrogenases. *Biochem Biophys Res Commun* **233**, 681–686.
- 23 Fischer M, Römisch W, Saller S, Illarionov B, Richter G, Rohdich F, Eisenreich W & Bacher A (2004) Evolution of vitamin B₂ biosynthesis: structural and functional similarity between pyrimidine deaminases of eubacterial and plant origin. *J Biol Chem* **279**, 36299–36308.
- 24 Bracher A, Eisenreich W, Schramek N, Ritz H, Gotze E, Herrmann A, Gutlich M & Bacher A (1998) Biosynthesis of pteridines. NMR studies on the reaction mechanisms of GTP cyclohydrolase I, pyruvoyltetrahydropterin synthase, and sepiapterin reductase. *J Biol Chem* 273, 28132–28141.
- 25 Scott LG, Tolbert TJ & Williamson JR (2000) Preparation of specifically 2H- and 13C-labeled ribonucleotides. Methods Enzymol 317, 18–38.
- 26 Bouhss A, Sakamoto H, Palibroda N, Chiriac M, Sarfati R, Smith JM, Craescu CT & Barzu O (1995) Enzymatic synthesis of guanine nucleotides labeled with ¹⁵N at the 2-amino group of the purine ring. *Anal Biochem* 225, 18–23.
- 27 Shaw E (1950) A new synthesis of the purines adenine, hypoxanthine, xanthine, and isoguanine. *J Biol Chem* 185, 439–447.
- 28 Bacher A, Richter G, Ritz H, Eberhardt S, Fischer M & Krieger C (1997) Biosynthesis of riboflavin: GTP cyclohydrolase II, deaminase, and reductase. *Methods Enzymol* 280, 382–389.
- 29 Laue TM, Shah BD, Ridgeway TM & Pelletier SL (1992) Computer-aided interpretation of analytical sedimentation data for proteins. In *Analytical Ultracentrifu*gation in Biochemistry and Polymer Science (Harding SE, Rowe AJ & Horton JC, eds), pp. 90–125. Royal Society of Chemistry, Cambridge.

Supporting information

The following supporting information is available: **Fig. S1.** Construction of a synthetic gene for 2,5-diamino-6-ribitylamino-4(3*H*)-pyrimidinone 5'-phosphate synthase of *A. aeolicus*.

Fig. S2. Boundary sedimentation and sedimentation equilibrium analysis of 2,5-diamino-6-ribitylamino-4(3*H*)-pyrimidinone 5'-phosphate synthase of *G. glabrata*.

Fig. S3. Sequence comparison of 2,5-diamino-6-ribitylamino-4(3*H*)-pyrimidinone 5'-phosphate synthases from *M. jannaschii*, *A. aeolicus* and *C. glabrata*.

Table S1. Oligonucleotides used for plasmid construction.

Table S2. *E. coli* strains and plasmids used in this study.

This supporting information can be found in the online version of this article.

Please note: Blackwell Publishing are not responsible for the content or functionality of any supporting information supplied by the authors. Any queries (other than missing material) should be directed to the corresponding author for the article.